Fisheries Research 191 (2017) 154–163

Contents lists available at ScienceDirect

Fisheries Research

journal homepage: www.elsevier.com/locate/fishres

Oceanographic determinants of ocean sunfish (*Mola mola*) and bluefin tuna (*Thunnus orientalis*) bycatch patterns in the California large mesh drift gillnet fishery

Nick Hahlbeck[a,*], Kylie L. Scales[b,c,d], Heidi Dewar[e], Sara M. Maxwell[f], Steven J. Bograd[b], Elliott L. Hazen[b,c]

[a] *Ernest F. Hollings Scholar, NOAA, USA*
[b] *NOAA Southwest Fisheries Science Center, Environmental Research Division, 99 Pacific Street Suite 255A, Monterey, CA 93950, USA*
[c] *Institute of Marine Sciences, University of California Santa Cruz, Santa Cruz, CA 95064, USA*
[d] *School of Science and Engineering, University of the Sunshine Coast, Maroochydore, QLD 4556, Australia*
[e] *NOAA Southwest Fisheries Science Center, Fisheries Resources Division,8901 La Jolla Shores Drive, La Jolla, CA 92037, USA*
[f] *Old Dominion University, Department of Biological Sciences,110 Mills Godwin Building, Norfolk, VA 23529, USA*

ARTICLE INFO

Article history:
Received 25 October 2016
Received in revised form 10 March 2017
Accepted 14 March 2017
Handled by Prof. George A. Rose

Keywords:
Bycatch
Ecosystem-based fisheries management
Dynamic ocean management
Bluefin tuna
Mola
Generalized additive model

ABSTRACT

The reduction of incidental capture of non-target species in a fishery (bycatch) is a key objective of ecosystem-based fisheries management (EBFM) and critical to the conservation of many marine species. Predicting bycatch events can inform targeted ecosystem-based management approaches to reduce risk. Here, the probability of ocean sunfish (*Mola mola*) and bluefin tuna (*Thunnus orientalis*) bycatch in the California large-mesh drift gillnet fishery is predicted using a suite of remotely-sensed environmental variables. Generalized additive models (GAMs) were used to model bycatch probability for these species in 8045 observed sets from 1990 to 2011, and predictive capabilities were assessed using *k*-fold cross validation. Bycatch probabilities for both species were elevated in regions of cool sea surface temperatures (<17 °C), likely related to seasonal upwelling dynamics in the California Current, a major eastern boundary upwelling ecosystem. *Mola* bycatch occurred primarily in late fall, at moderate eddy kinetic energy values (0.006–0.008 m^2/s^2) and in areas of high seafloor rugosity. Bluefin tuna bycatch rates were higher west of the Southern California Bight, also in late fall, and appear to be associated with the seasonal upwelling frontal zone. These models can be used with near-real time satellite data by both fishers and managers for bycatch avoidance, providing a tool for more dynamic ocean management strategies.

1. Introduction

Ecosystem-based fisheries management (EBFM) is a holistic approach towards maximizing sustainability in fisheries, but effective EBFM implementation requires better understanding of the complex trophic and environmental interactions that sustain a given ecosystem (Essington et al., 2015; Lindegren et al., 2009; Large et al., 2015). Advances in remote sensing technologies and modeling techniques have created valuable tools to help characterize those interactions. These tools have generated interest in dynamic management strategies that incorporate near-real-time model predictions based on dynamic oceanographic variables (Hobday and Hartog, 2014; Maxwell et al., 2015). When *in situ* data are collected at spatiotemporal ranges and resolutions that are insufficient for prediction, a comparative wealth of remotely-sensed data can often be used in addition to (e.g. Nakada et al., 2014) or instead of (e.g. Reiss et al., 2008) *in situ* data. In many cases, models using remotely-sensed data have been shown to match or surpass the predictive capability of their *in-situ*-only counterparts in predicting important oceanographic features and species habitat preferences (Takano et al., 2009; Becker et al., 2010; Palamara et al., 2012).

One application of habitat-based models in EBFM is reducing incidental catch of non-target species. Bycatch mitigation is of particular interest due to the potential for negative ecological (Zhang et al., 2016) and economic (Kasperski, 2016) impacts on fisheries. Models incorporating near-real-time dynamic ocean variables hold potential as an important component of bycatch mitigation strategies (Lewison et al., 2015). Hartog et al. (2010) demonstrated

* Corresponding author at: Department of Fisheries and Wildlife, Oregon State University, 104 Nash Hall, Corvallis, OR 97331, USA.
E-mail address: nicholas.hahlbeck@oregonstate.edu (N. Hahlbeck).

http://dx.doi.org/10.1016/j.fishres.2017.03.011
0165-7836/

© 2017 published by Elsevier. This manuscript is made available under the Elsevier user license
https://www.elsevier.com/open-access/userlicense/1.0/

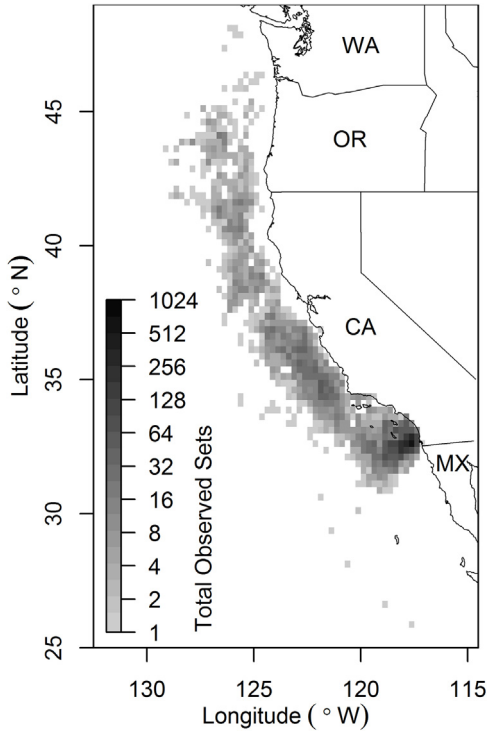

Fig. 1. Spatial distribution of cumulative effort (observed sets) in the California commercial drift gillnet fishery from 1990 to 2011. Coastal administrative boundaries are provided for spatial reference (WA = Washington; OR = Oregon; CA = California; MX = Mexico). Darker areas indicate higher fishing effort; white indicates no effort.

that yellowfin (*Thunnus albacares*) and Southern bluefin (*Thunnus maccoyii*) tuna stocks can be separated in space and time using models to predict environmentally-driven variation in habitat overlap. In addition, Dunn et al. (2016) showed that Atlantic cod (*Gadus morhua*) fisheries achieved lower bycatch ratios when using dynamic approaches to direct fishing activity.

Ocean sunfish (*Mola mola*) and Pacific bluefin tuna (*Thunnus orientalis*) are incidentally caught in the limited-entry California commercial large mesh, drift gillnet (CA DGN) fishery. The fishery was founded on harvest of common thresher shark (*Alopias vulpinus*) off the entire United States West Coast, but in the early years of the fishery broadbill swordfish (*Xiphias gladius*) replaced common thresher as the primary target. A number of time-area closures have been added over the years to protect a variety of species, particularly pregnant thresher sharks and endangered leatherback (*Dermochelys coriacaea*) and loggerhead (*Caretta caretta*) sea turtles (Carretta et al., 2014). As a result of these management measures, the extent and magnitude of effort have decreased dramatically over time; beginning after the leatherback closure in 2001, effort became confined primarily to the Southern California Bight from October–December, while cumulative effort encompasses a greater spatiotemporal range (Fig. 1).

While large numbers of finfish are incidentally caught in the CA DGN fishery, they have received less attention than protected species with regards to bycatch reduction. *Mola* comprise the largest catch of any single species in the CA DGN fishery at more than 2500 individuals per year in observed sets from 1990 to 2011, which is more than three times the target catch of swordfish (NMFS, 2016). In addition, approximately 190 bluefin tuna were caught per year in observed sets during this time period, totaling nearly one-fourth of swordfish catch by number of individuals. Though both species are considered incidental catch, most bluefin are retained and sold while 95% of *Mola* are released alive, although post-release survival is unknown (Thys et al., 2015). Though *Mola* mortality from the fishery is thought to be low, *Mola* comprise a large fraction of total catch in California (Cartamil and Lowe, 2004) and other drift gillnet fisheries worldwide (e.g. Silvani et al., 1999; Akyol et al., 2005) which provides a motive for understanding factors contributing to their high bycatch rates. Bluefin tuna are commercially valuable and populations are overfished (ISC, 2016); thus even moderate bycatch of this species is of particular interest to management and conservation efforts.

Both *Mola* and bluefin tuna use the California Current Large Marine Ecosystem (CCLME) as a foraging ground. Environmental conditions in the area of the CCLME targeted by the fishery are dominated by seasonally and locally variable upwelling systems. Upwelling tends to be stronger, though more variable, with increasing latitude, and the duration of the season decreases from nearly year-round off Southern California to spring and summer months off the Washington coast (Bograd et al., 2009; Black et al., 2011). Tracking studies suggest that both *Mola* (Thys et al., 2015) and bluefin tuna (Boustany et al., 2010) associate with these productive upwelling zones in the CCLME. This upwelling association is expected to play a major role in bycatch rates for both species; however, differences in foraging strategies may yield different relationships with similar environmental factors. Bluefin feed primarily on fish, squid and crustaceans (Pinkas et al., 1971) while *Mola* feed on jellyfish (Fraser-Brunner, 1951). This study seeks to identify key environmental influences on bycatch rates of *Mola* and bluefin tuna in the CA DGN fishery, ultimately to inform dynamic bycatch reduction models.

2. Methods

Catch data were collected from the CA DGN fishery through the NMFS West Coast Region Observer program from 1990 to 2011. A range of data were recorded for the 8045 observed sets, including date, soak time, coordinates, number of individuals of each species caught and their disposition if released. Of these, 12 outliers with soak times >3 sd from the mean (greater than 21 h) and one set with a missing soak time were excluded, and soak time was not considered as a variable in further analysis. Number of *Mola* and bluefin tuna caught was converted to presence or absence for each set with bycatch rate for a given time or spatial stratum being defined as the proportion of sets with positive catch. *Mola* and bluefin tuna were present in approximately 75% and 12.5% of total sets from 1990 to 2011 respectively. Observer coverage for the catch dataset was approximately 15% of all sets within the fishery for 1990–2011 (Martin et al., 2015). A variogram was used to assess spatial autocorrelation (rgdal, sp and gstat packages for R 3.2.1; Bivand et al., 2016; Bivand et al., 2013; Pebesma and Bivand, 2005; Pebesma, 2004; R Core Team, 2015) and the maps, mapdata and raster packages for R (Becker et al., 2015a,b; Hijmans, 2015) were used to visualize specific patterns in spatially autocorrelated bycatch data.

A suite of remotely-sensed environmental variables, including sea surface temperature (SST), chlorophyll-*a* concentration, zonal and meridional geostrophic velocities, sea surface height anomaly (SSH-a), zonal and meridional wind vectors and bathymetry, was downloaded from the NOAA ERDDAP server (Simons, 2015). These data were paired spatially and temporally with each set. Several derived variables were also calculated from the raw data. The standard deviations of bathymetry and SST were used as indices of rugosity and spatial variation in temperature respectively. Eddy kinetic energy (EKE) was calculated from the geostrophic current anomalies. The resolutions and sources for all remotely-sensed variables are summarized in Table 1. Month and latitude-longitude coordinates for each set were also considered as variables.

To address zero-inflation and autocorrelation among consecutive sets, data were aggregated by month. Binary bycatch data for

Table 1
Remotely-sensed variables used in construction of *a priori Mola* and bluefin tuna bycatch models. The original data source, spatiotemporal resolution, temporal availability and percent coverage of 8045 total gillnet sets are provided for each variable. A dash (–) indicates the specified value is not applicable to the specified variable. An asterisk (*) denotes variables affected by clouds.

Variable	Source	URL	Temporal Resolution	Spatial Resolution	Temporal Availability	Coverage of Total Sets
Sea Surface Temperature (SST)*	Pathfinder AVHRR, Ver. 5.0, Global	http://coastwatch.pfeg.noaa.gov/erddap/info/erdPHssta8day/index.html	8-day	0.044°	Jul 1990–Dec 2007	89%
SST Spatial Variability*	St. dev. of SST	(above)	8-day	0.044°	(above)	88%
Sea Surface Height Anomaly (SSH-*a*)	AVISO Maps of Sea Level Anomaly: Height (MSLA-H), Global	http://coastwatch.pfeg.noaa.gov/erddap/info/erdTAssh1day/index.html	1-day	0.25°	Oct 1992–Dec 2012	74%
Eddy Kinetic Energy (EKE)	Derived from AVISO UV Maps of Geostrophic Velocity Anomalies (MSLA-UV), Global: $½(u^2+v^2)$	http://coastwatch.pfeg.noaa.gov/erddap/info/erdTAgeo1day/index.html	1-day	0.25°	Oct 1992–Dec 2012	72%
Chlorophyll-*a**	SeaWIFS Orbview-2, Global	http://coastwatch.pfeg.noaa.gov/erddap/info/erdSWchla8day/index.html	8-day	0.1°	Sept 1997–Dec 2010	42%
Wind Velocity	QuikSCAT SeaWinds, Global	http://coastwatch.pfeg.noaa.gov/erddap/info/erdQSwind3day/index.html	3-day	0.1°	Jul 1999–Nov 2009	35%
Bathymetry	ETOPO1 Topography, Ice Sheet Surface version, Global	http://coastwatch.pfeg.noaa.gov/erddap/info/etopo360/index.html	–	0.017°	–	100%
Seafloor rugosity	St. dev. of bathymetry	(above)	–	0.017°	–	100%

Mola and bluefin tuna were converted to a monthly proportion of sets with non-zero bycatch, and the results were paired with the mean of each environmental variable for the corresponding month ($n = 143$). Multicollinearity among the predictor variables was assessed by calculating the variance inflation factor (VIF) for each monthly aggregated variable. All VIF values except latitude (7.0) and longitude (13.0) were below the recommended threshold of 3.0 (Zuur et al., 2009). If either longitude or latitude were removed from the predictor dataset, the VIF of the other was less than 4.0; thus, longitude and latitude were never used in the same model. Six EKE outlier values from a region of poor sampling density (>2.5 standard deviations from the mean) were removed from the dataset due to disproportionately high influence on model performance in all but one of the model candidates.

Based on preliminary exploration of the aggregated dataset and the ecological literature for each species, 12 *a priori* model candidates were constructed for each species using generalized additive models (GAMs). GAMs have been used successfully to model both bycatch (Martinez-Rincon et al., 2015; Zydelis et al., 2011) and habitat preferences (Becker et al., 2010; Stoner et al., 2001) of marine species, as well as ecological indicators (Large et al., 2015) using environmental predictor variables. Each model candidate was fitted using a binomial family with a logistic link function and data were weighted according to monthly sample size using the mgcv 1.8.6 package in R (Wood, 2006). In addition to *a priori* model construction, the monthly aggregated data were used for assessment of possible correlation between bycatch rate and the regime of the Pacific Decadal Oscillation (PDO) determined from the summer PDO index (Mantua et al., 1997). Based on the negative correlation between the PDO and upwelling across the United States West Coast (Macias et al., 2012) and an expected effect of upwelling association on bycatch rates in both species, a Mann-Whitney *U* test was used to compare bycatch rates of each species during positive (warm) and negative (cool) PDO regimes.

To reduce problems with stepwise model selection such as high frequency of noise variables (Lukacs et al., 2010; Derksen and Keselman, 1992) and multiple hypothesis testing (Whittingham et al., 2006), a *k*-fold cross validation approach ($k = 100$) was used to select a final model. Data points were divided randomly into a training set (80%) and a testing set (20%) and the model was "trained" (fit to the training set only). The trained model was then used to predict the response from the testing set. This process was repeated 100 times, and a least-squares linear regression of observed vs. median predicted response was performed. The final model was chosen using the slope and r^2 of this regression (hereafter denoted b_p and $r_p{}^2$) as predictive performance metrics.

3. Results

A variogram of monthly *Mola* bycatch rates across the entire timespan of the dataset (1990–2011) revealed nearly constant variance with respect to distance between sets, indicating little spatial autocorrelation in *Mola* bycatch. Distributions of high and low *Mola* bycatch were essentially homogeneous across the spatial extent of fishing effort (Fig. 2). In contrast, bluefin tuna bycatch exhibited an asymptotic threefold increase in variance with increasing distance between sets. Most high bycatch rates occurred along a linear band roughly parallel to the coast, extending from inshore waters near Central California to 150–200 km offshore in the Southern California Bight (Fig. 3). Monthly distributions of bycatch rate revealed annual peaks late in the season for both species that generally aligned with fishing effort, with maximum *Mola* bycatch in November-January and maximum bluefin tuna bycatch in October-December (Fig. 4). Annual peak bycatch rate exceeded 0.9 for *Mola* nearly every year (median = 0.73), while peak bluefin tuna bycatch rate displayed higher interannual variation (approx. 0.1–0.4; median = 0.07; Fig. 5). Correlation between the regime of the Pacific Decadal Oscillation (PDO) and bluefin tuna bycatch rate proved significant (warm regime median 0.04; cool regime median 0.1; $p < 0.05$); in contrast, *Mola* bycatch rate exhibited no such correlation (warm regime median 0.74; cool regime median 0.73; $p > 0.05$).

The final *Mola* bycatch model included month, EKE, SST and rugosity as predictor variables ($r_p{}^2 = 0.52$; $b_p = 0.58$; 63% deviance explained). The model indicated a strong increase in bycatch probability over the course of the fishing season, though the period of maximum predicted bycatch probability preceded the observed maximum in monthly distributed bycatch rates by approximately 1 month. Higher bycatch probability was also predicted in areas of cool surface waters (<17 °C) relative to the range encountered by the fishery (14–22 °C; Fig. 6). The model further suggested that bycatch probability is higher in areas with moderate EKE val-

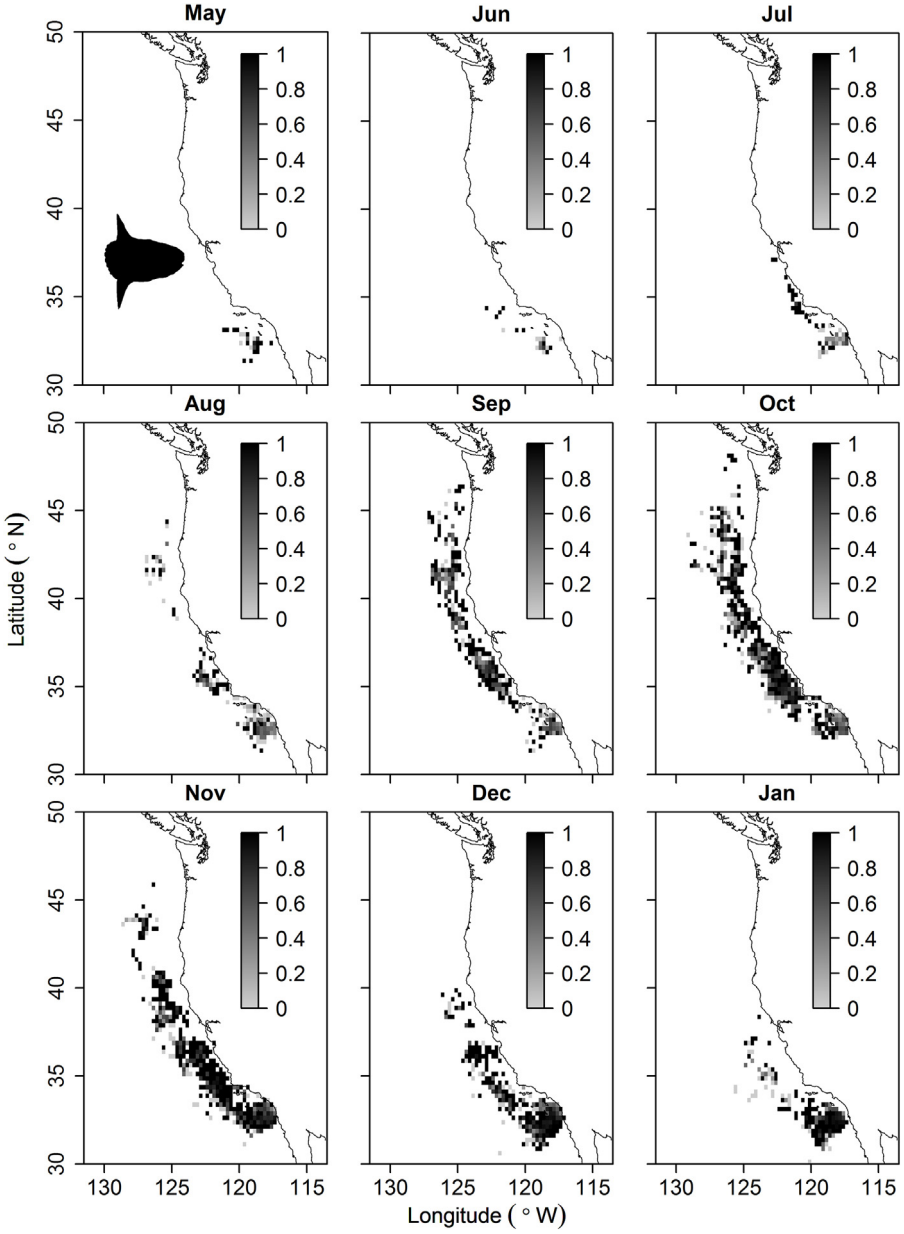

Fig. 2. Spatial distribution of *Mola* bycatch rate from 1990 to 2011. Bycatch rate is defined as the fraction of total sets within that cell containing at least one individual. Darker grid cells indicate higher bycatch rate, expressed in probability units (0–1). Grid cells are 0.25° squares. The black line indicates the Pacific coast of North America.

ues (0.006–0.008 m^2/s^2) and high rugosity (175–225 m) relative to the full ranges of these parameters (0–0.016 m^2/s^2 and 80–270 m respectively), though these effects were less pronounced. One other candidate model performed similarly to the final model during validation ($r_p{}^2 = 0.51$; $b_p = 0.62$; 67.5% deviance explained) and included the same predictor variables plus chlorophyll-*a* concentration. Chlorophyll-*a* data coverage was sparse compared to other variables (see Table 1), and its inclusion in the model reduced the sample size of monthly aggregated data from $n = 92$ to $n = 66$. The low effect size for chlorophyll-*a* and similar smooths for other included variables at the cost of this large reduction in sample size was the basis for rejection of this model in favor of the final model. Comparison of the final model with ($n = 98$) and without EKE outliers indicated negligible difference between all corresponding smooths outside of the removed values.

The final bluefin tuna bycatch model included EKE, SST, chlorophyll-*a* concentration and longitude ($r_p{}^2 = 0.53$; $b_p = 0.56$; 72% deviance explained). Compared with the *Mola* model, high bluefin tuna bycatch was similarly observed at low SST (<17 °C) and moderate EKE (0.005-0.007 m^2/s^2), though EKE exhibited a smaller effect size on bycatch of bluefin tuna than *Mola* (Fig. 7). Higher bycatch probabilities were predicted west of the Southern California Bight (>119°W), and in regions with low surface chlorophyll-*a* concentrations (<0.3 mg/L) compared to the range of conditions encountered by the fishery (117−123°W and 0.0–1.0 mg/L respectively). A slight increase in bycatch probability was also predicted for the upper range of chlorophyll-*a* concentrations (0.8–1.0 mg/L) but 95% confidence intervals indicate this prediction is highly uncertain due to low sampling density in this region.

4. Discussion

Avoiding harmful interactions with non-target species while maintaining sustainable target species catch is both a formidable challenge and a crucial step towards successful EBFM. Complex models that link incidental catch data to environmental conditions

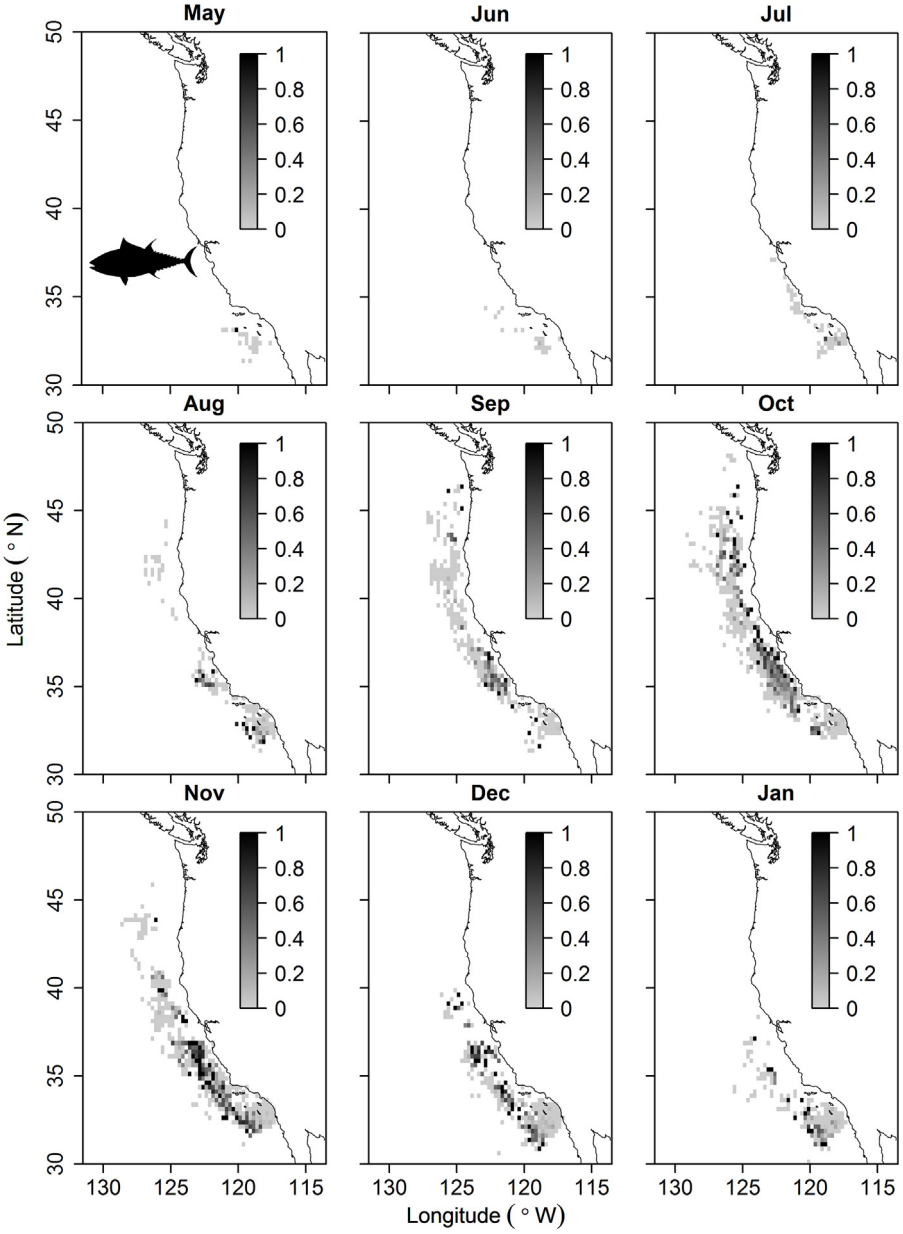

Fig. 3. Spatial distribution of bluefin tuna bycatch rate from 1990 to 2011. Bycatch rate is defined as the fraction of total sets within that cell containing at least one individual. Darker grid cells indicate higher bycatch rate, expressed in probability units (0–1). Grid cells are 0.25° squares. The black line indicates the Pacific coast of North America.

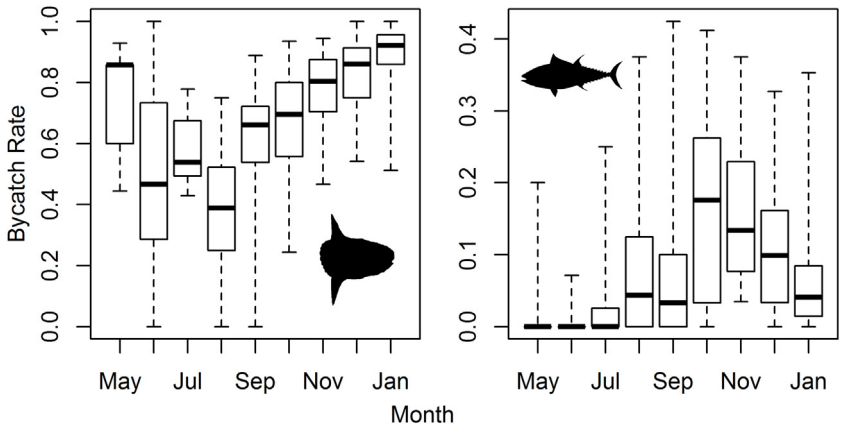

Fig. 4. Monthly distributions of *Mola* (left) and bluefin tuna (right) bycatch rates from 1990 to 2011. Bycatch rate is defined as the fraction of total sets per month containing at least one individual. The dark bar, top and bottom box edges and dotted line ends represent the median, 75th and 25th percentiles and range respectively.

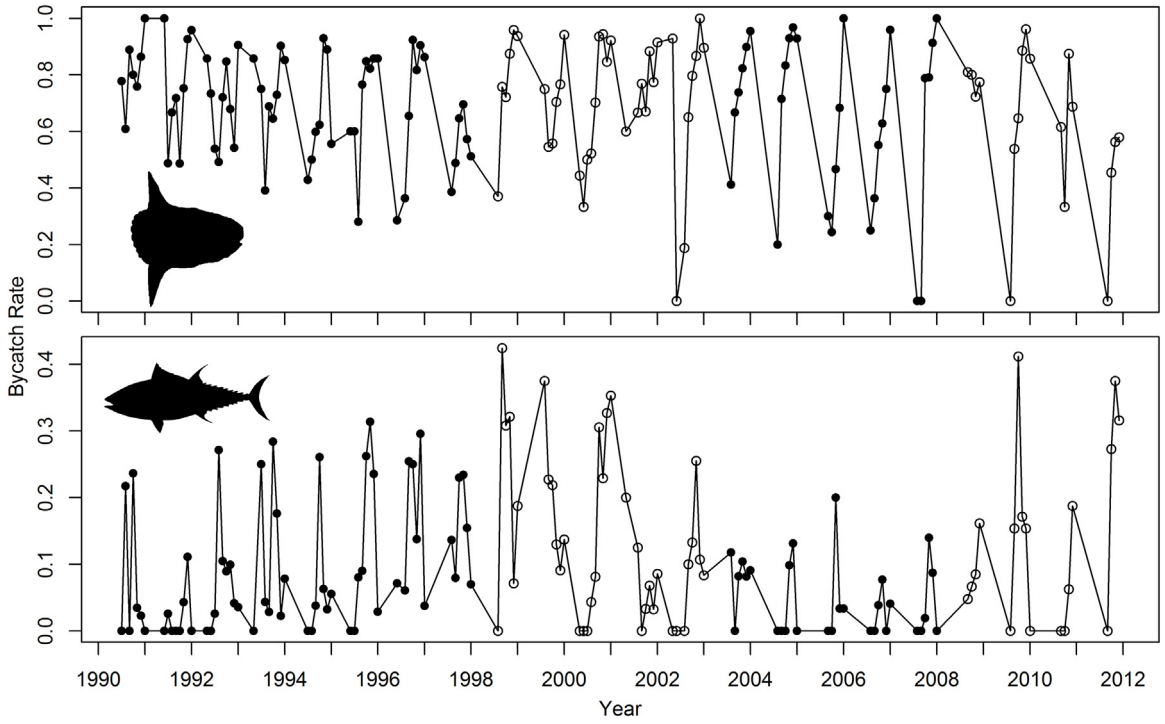

Fig. 5. Time series of monthly aggregated bycatch rate for *Mola* (top) and bluefin tuna (bottom). Bycatch rate is defined as the fraction of total sets per month containing at least one individual. The closed and open circles correspond to the regime of the Pacific Decadal Oscillation (PDO; Mantua et al., 1997). Closed and open circles indicate years of positive (warm) and negative (cool) PDO regimes respectively.

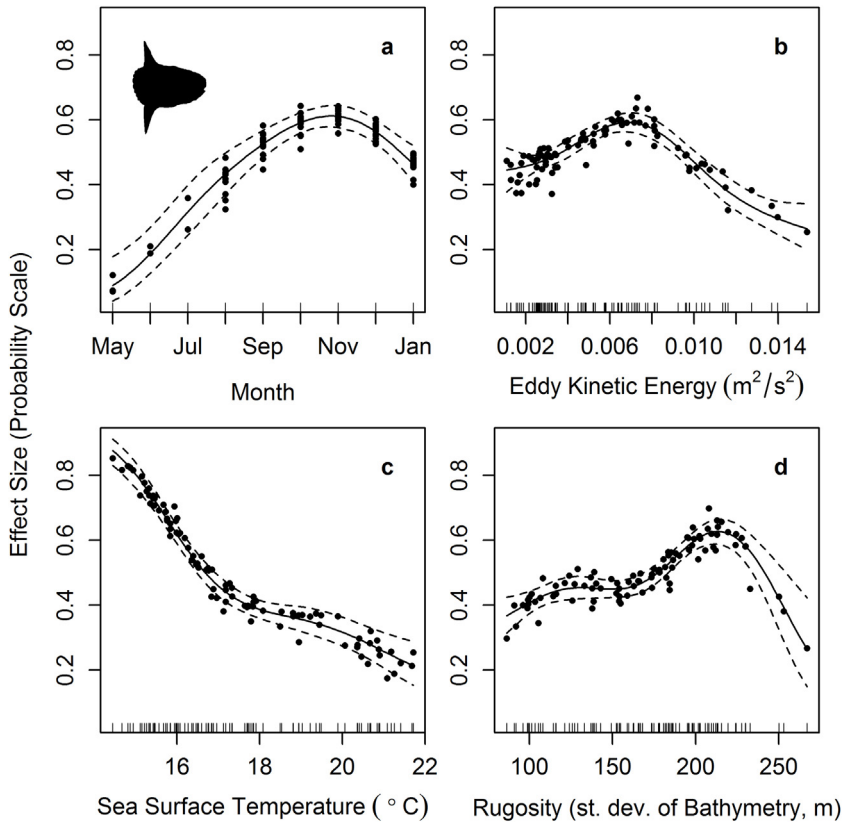

Fig. 6. Smooth functions for variables from the final *Mola* bycatch model, including (a) month, (b) EKE, (c) SST and (d) seafloor rugosity. Effect size for each variable is expressed in probability units (0–1) and indicates the individual contribution of that variable to total bycatch probability. Dashed lines indicate upper and lower 95% confidence intervals. Tick marks above the x-axis indicate sampling density across the independent variable range. Sampling density of the "month" variable is described in more detail in Supplemental Materials.

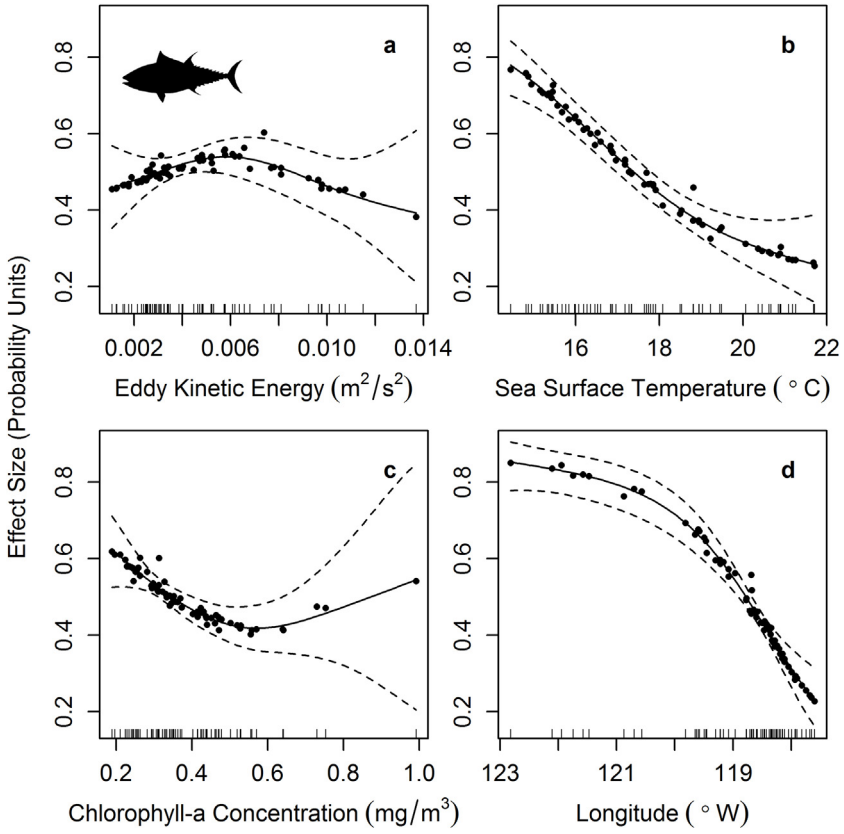

Fig. 7. Smooth functions for variables from the final bluefin tuna bycatch model, including (a) EKE, (b) SST, (c) chlorophyll-*a* and (d) longitude. Effect size for each variable is expressed in probability units (0–1) and indicates the individual contribution of that variable to total bycatch probability. Dashed lines indicate upper and lower 95% confidence intervals. Tick marks above the x-axis indicate sampling density across the independent variable range.

have the potential to be an effective tool for reducing bycatch in marine fisheries. The potential to predict the distribution of bycatch in near-real time opens the door to dynamic management based on oceanographic conditions rather than static time-area closures that may be unnecessarily restrictive and reduce fishing opportunity and economic viability (Hobday and Hartog, 2014; Maxwell et al., 2015; Lewison et al., 2015). The majority of studies modeling bycatch have focused on protected species (e.g. Zydelis et al., 2011; Martin et al., 2015). We apply the same tools to finfish and broaden the scope of bycatch reduction efforts and EBFM.

Bycatch rates of *Mola* in the CA DGN fishery exhibit low interannual variability and are higher in fall to early winter, in cooler sea surface temperatures (<17° C) and in association with complex seafloor topography. These associations imply a link with upwelling in the CCLME. Upwelling of cool, nutrient-rich waters likely provides the main source of primary productivity to sustain the growth of gelatinous zooplankton populations upon which *Mola* prey (Ware and Thomson, 2005). Areas with abrupt topographic change and moderate EKE values within the approximate depth range represented in the final model (1537 ± 611 m; mean ± sd) could provide a physical environment conducive to zooplankton concentration (Santora et al., 2012; Genin, 2004; Graham et al., 2001) which in turn provides forage for these gelatinous zooplankton. The timing of high predicted bycatch rates corresponds to the later upwelling season across much of California (Bograd et al., 2009) which could indicate a time lag from the seasonal maximum required for sufficient trophic transfer of upwelled nutrients to support large gelatinous zooplankton aggregations. Alternatively, *Mola* could spend the earlier upwelling season taking advantage of seasonal jellyfish blooms in other highly productive areas, such as *Chrysaora spp*. in the Northeast Pacific during July–September (Suchman et al., 2012).

Mola are known to associate with fronts and display vertical migratory behavior, foraging in association with the deep-scattering layer along frontal boundaries where zooplankton often concentrate (e.g. Dewar et al., 2010; Nakamura et al., 2015; Sousa et al., 2016; Cartamil and Lowe, 2004). Thys et al. (2015) used an individual with a Fastloc GPS tag to analyze association with fine-scale ocean features and found that tag locations matched the cold side of a front peripheral to an upwelling zone. The lack of a significant relationship with spatial variability of SST in this study was probably due to its crudeness as an indicator of complex frontal structure that tends to occur on shorter time scales, and a more targeted metric may yield an association similar to those described elsewhere (e.g. Miller et al., 2015; Scales et al., 2014). Though the model exhibited no direct evidence of frontal association, the link to upwelling indicated by the model combined with greater bycatch probability at moderate EKE values may suggest a possible increase in *Mola* bycatch risk near upwelling-derived frontal areas.

Similar to *Mola*, the temperature relationship in the bluefin tuna model is also likely indicative of an association with upwelling. This link to SST is corroborated by tracking studies documenting fall migrations of bluefin tuna to cold waters off Point Conception and Monterey Bay (Boustany et al., 2010; Kitagawa et al., 2007). In these studies, the arrival of bluefin tuna in these waters generally coincided with the final days of major upwelling events, and their departure often followed coastal advection of warm water due to downwelling. High feeding rates indicated by internal-external temperature ratios are known to occur during this time period (Kitagawa et al., 2007; Whitlock et al., 2015), suggesting at least

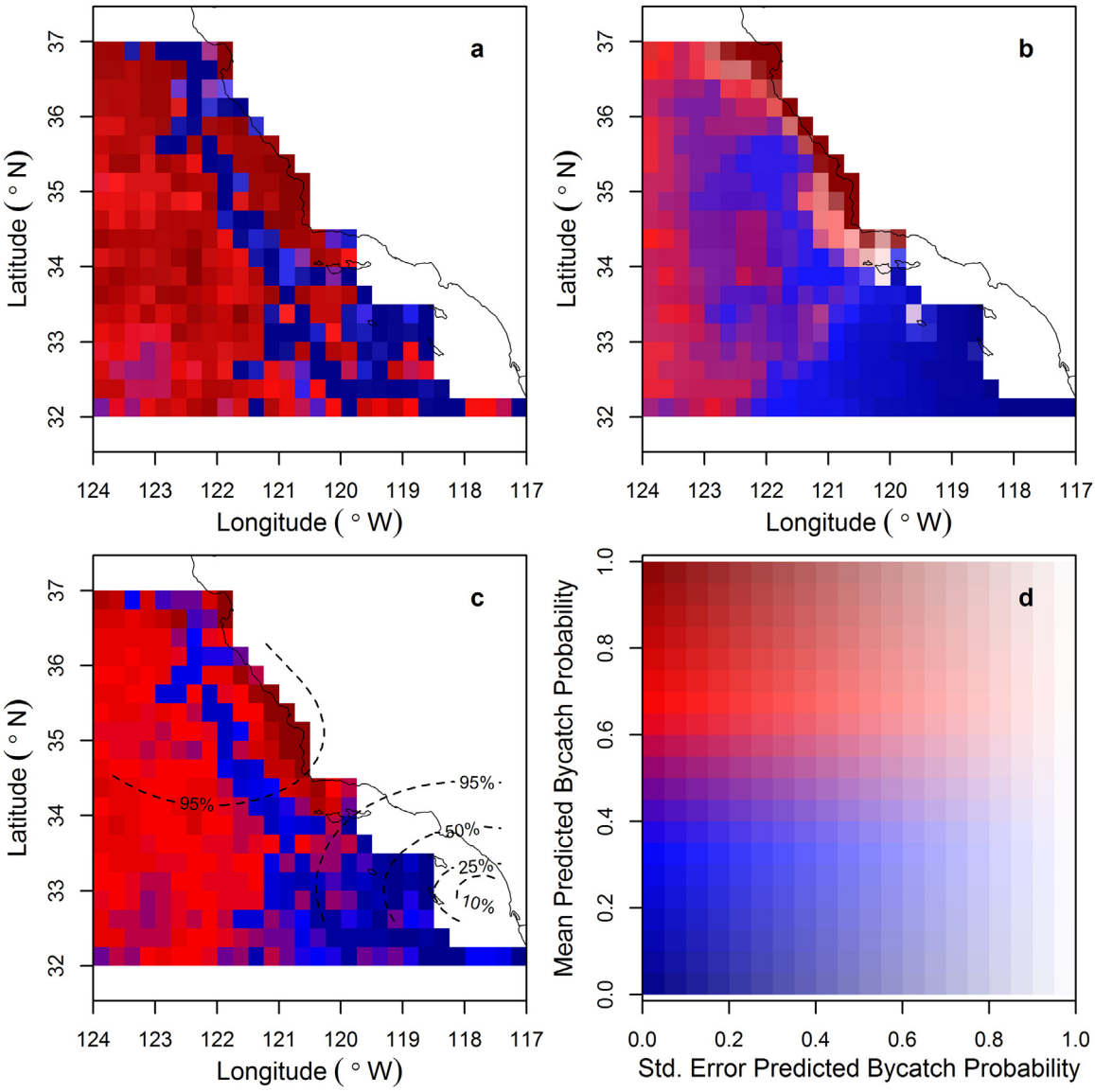

Fig. 8. Example bycatch prediction surfaces for November 2006 for (a) *Mola*, (b) bluefin tuna and (c) both species based on the final models. In the single-species plots, color indicates mean predicted bycatch probability while transparency indicates estimated standard error according to (d). The multi-species plot exemplifies an integrated bycatch risk map; color indicates the mean of bycatch probability predictions for both species (this mean could be weighted differently to reflect species-specific management priorities, but is weighted evenly here). Standard error (transparency) is not included in the multi-species plot. Dotted lines indicate kernel density contours of fishing effort for November 2006. The solid black line indicates the Pacific coast of North America.

partial dependence on upwelling-induced productivity that contributes to greater bycatch risk near upwelling zones.

In comparison to *Mola*, bluefin tuna bycatch probabilities exhibited a greater degree of spatial variation and bluefin appear to have a stronger association with the seasonal upwelling frontal zone. Supporting evidence for this comes from other studies on tuna distributions. Laurs et al. (1984) found that nearly all albacore tuna (*Thunnus alalunga*) catch in the California Current during a two-month period occurred along the offshore side of an upwelling-derived frontal boundary; this region was characterized by low phytoplankton pigment concentration and temperatures colder than the nearby coastal waters of the Southern California Bight (18–20 °C) but warmer than the upwelling zone (10–12 °C). Similarly, the increase in bycatch probability predicted by the model in areas further west, with low chlorophyll-*a* and temperatures <17 °C, may indicate that the waters just offshore from an upwelling frontal boundary provide conditions favorable to bluefin tuna as well. Additionally, the region of high bycatch corresponds well to areas of maximum frontal occurrence identified in other studies (Powell and Ohman, 2015; Lynn and Simpson, 1987). Frontal zooplankton concentrations that could support schools of forage fish combined with clear, low-chlorophyll water could facilitate foraging for visual predators such as tunas (Murphy, 1959). The potential dependence of foraging bluefin tuna on upwelling-derived fronts in the CCLME would provide a plausible explanation for both the oceanographic relationships described by the model and the spatial bycatch patterns observed in this study.

The association with seasonal upwelling and upwelling-derived fronts indicated by the models does explain variation in bycatch rate of both species on monthly timescales, but variations on longer timescales likely depend on additional complex interactions not predicted by the model. For example, the PDO is thought to influence nutrient availability through structural changes in coastal upwelling cells during contrasting phases (Chhak and Di Lorenzo, 2007). The apparent response of only bluefin tuna bycatch rates to PDO regime shifts suggests that the relationships of both *Mola*

and bluefin bycatch to upwelling alone are insufficient to explain multi-annual patterns in these species' interactions with the CA DGN fishery. One possible additional factor may be PDO-linked changes in community structure at several trophic levels (Du et al., 2015; Zwolinski and Demer, 2014). Differences in trophic relationships among species could alter the nature of individual species' relationships to upwelling in the context of a new community structure. A second explanation may be shifts in the distribution of bluefin across the North Pacific. Decadal-scale environmental variability has been linked to bluefin recruitment and the number of fish that make the West-East trans-Pacific migrations (Polovina, 1996; Sakuramoto, 2016). Further investigation into the complex ties between large-scale climate indices, mesoscale ocean features and species life-history traits would improve the ability of bycatch models to capture variation at multiple spatial and temporal scales.

The results of this study illustrate the potential utility of remotely sensed dynamic variables in understanding patterns of fisheries bycatch. The models exhibited relatively high prediction accuracy ($r_p^2 > 0.5$) and explained more than 60–70% of variability in incidental catch of *Mola* and bluefin tuna. With continued improvements in resolution and coverage of remotely sensed variables and derived products that better describe dynamic ocean features such as fronts, this type of model could become a valuable tool for ecosystem management through predictions of integrated bycatch risk for multiple species in conjunction with target catch (Fig. 8). Additional data collection to better represent the current state of the entire fishery would also be beneficial to model improvement. Observer placement is subject to vessel size, which may introduce bias in terms of fishing location and practice. In addition, the redistribution of fishing effort following major management changes necessitates an examination of how fishery characteristics affect bycatch rates and likely add variability unexplained by the model.

Currently, the CA DGN fishery is managed using multiple spatiotemporal closures and gear restrictions to reduce turtle and cetacean bycatch, but little attention has been focused on large teleost fish species. Examining bycatch patterns of multiple species allows us to better understand tradeoffs, and ensure that our management solutions do not create new problems. For example, it is unknown whether the high *Mola* bycatch risk predicted in late fall is an effect of peak effort timing alone, or whether higher fishing pressure may be compounding the effect of other seasonal influences on bycatch risk. The results of this study also suggest increased bluefin tuna bycatch risk in specific areas 150–200 km offshore during October-December, partially overlapping maximum *Mola* bycatch risk in space and time. Therefore, these models could inform more targeted tools for dynamic ocean management, such as dynamic area closures based on integrated bycatch ratio predictions for multiple species, or dynamic seasonal closures based on changes in environmental conditions and community structures rather than calendar months. Important to the success of these approaches would be the addition of model predictions for the catch of target species as well (e.g. Ward et al., 2015; Dunn et al., 2016; Watson et al., 2009).

Advancing dynamic tools for integration into current management strategies is a crucial step towards improving EBFM and reducing bycatch, which is a key mandate in the Magnuson-Stevens Fisheries Conservation and Management Act. In the CA DGN fishery, *Mola* are caught at three times the rate of swordfish, despite holding no commercial value. Pacific bluefin tuna also comprise a significant component of incidental catch in the fishery at one-fourth the total catch of swordfish despite having been reduced to less than 4% of their unfished biomass across the Pacific (ISC, 2016). Consequently, development of bycatch models that could inform management efforts is of significant interest. The relatively high prediction accuracy shown in this case study suggests that multi-species bycatch prediction models have the potential to help to inform ecosystem management in the CA DGN fishery. Broader application of these models to global bycatch concerns across gear types could help reduce unwanted catch of additional species and ultimately improve the sustainability of fisheries.

Acknowledgements

N.H. wishes to thank K&KH, the NOAA Hollings Scholarship program and the NMFS Environmental Research Division for their support. The authors also wish to thank the fishermen and observers from the CA DGN fleet involved in data collection. Funding for the broader project was provided by grants from NOAA's Bycatch Reduction and Engineering Program grant ['Real-time fisheries management for ecological and economic sustainability'] and NASA's Ecological Forecasting [grant number NNH12ZDA001N-ECOF].

Appendix A. Supplementary data

Supplementary data associated with this article can be found, in the online version, at http://dx.doi.org/10.1016/j.fishres.2017.03.011.

References

Akyol, O., Erdem, M., Unal, V., Ceyhan, T., 2005. Investigations on drift-net fishery for swordfish (Xiphias gladius L.) in the Aegean Sea. Turk. J. Vet. Anim. Sci. 29 (6), 1225–1231.

Becker, E., Forney, K., Ferguson, M., Foley, D., Smith, R., Barlow, J., Redfern, J., 2010. Comparing California Current cetacean–habitat models developed using in situ and remotely sensed sea surface temperature data. Mar. Ecol. Prog. Ser. 413, 163–183.

Becker, R., Wilks, A., Brownrigg, R., Minka, T., 2015a. Maps: draw geographical maps. R package version 2., pp. 3–10 http://CRAN.R-project.org/package=maps.

Becker, R., Wilks, A., Brownrigg, R., Minka, T., 2015b. Mapdata: extra map databases R package version 2., pp. 2–4 http://CRAN.R-project.org/package=mapdata.

Bivand, R., Pebesma, E., Gomez-Rubio, V., 2013. Applied Spatial Data Analysis with R, 2nd ed. Springer, NY http://www.asdar-book.org/.

Bivand, R., Keitt, T., Rowlingson, B., 2016. Rgdal: bindings for the geospatial data abstraction library R package version 1., pp. 1–10 http://CRAN.R-project.org/package=rgdal.

Black, B., Schroeder, I., Sydeman, W., Bograd, S., Wells, B., Schwing, F., 2011. Winter and summer upwelling modes and their biological importance in the California Current Ecosystem. Global Change Biol. 17, 2536–2545.

Bograd, S., Schroeder, I., Sarkar, N., Qiu, X., Sydeman, W., Schwing, F., 2009. Phenology of coastal upwelling in the California Current. Geophys. Res. Lett. 36 (1), L01602.

Boustany, A., Matteson, R., Castleton, M., Farwell, C., Block, B., 2010. Movements of pacific bluefin tuna (Thunnus orientalis) in the Eastern North Pacific revealed with archival tags. Prog. Oceanogr. 86, 94–104.

Carretta J., Enriquez L., Villafana C., (eds.) 2014. Marine mammal, sea turtle and seabird bycatch in California gillnet fisheries in 2012. NOAA Technical Memorandum NMFS-SWFSC-526, 16 p.

Cartamil, D., Lowe, C., 2004. Diel movement patterns of ocean sunfish Mola mola off Southern California. Mar. Ecol. Prog. Ser. 266, 245–253.

Chhak, K., Di Lorenzo, E., 2007. Decadal variations in the California Current upwelling cells. Geophys. Res. Lett. 34 (14), L14604.

Derksen, S., Keselman, H., 1992. Backward, forward and stepwise subset selection algorithms: frequency of obtaining authentic and noise variables. Br. J. Math. Stat. Psychol. 45, 265–282.

Dewar, H., Thys, T., Teo, S., Farwell, C., O'sullivan, J., Tobayama, T., Soichi, M., Nakatsubo, T., Kondo, Y., Okada, Y., Lindsay, D., Hays, G., Walli, A., Weng, K., Streelman, J., Karl, S., 2010. Satellite tracking the world's largest jelly predator, the ocean sunfish, Mola mola, in the Western Pacific. J. Exp. Mar. Biol. Ecol. 393 (1-2), 32–42.

Du, X., Peterson, W., O'Higgins, L., 2015. Interannual variations in phytoplankton community structure in the northern California Current during the upwelling seasons of 2001–2010. Mar. Ecol. Prog. Ser. 519, 75–87.

Dunn, D., Moxley, J., Halpin, P., 2016. Temperature-based targeting in a multispecies fishery under climate change. Fish. Oceanogr. 25 (2), 105–118.

Essington, T., Baskett, M., Sanchirico, J., Walters, C., 2015. A novel model of predator-prey interactions reveals the sensitivity of forage fish: piscivore fishery trade-offs to ecological conditions. ICES J. Mar. Sci. 72 (5), 1349–1358.

Fraser-Brunner, A., 1951. The ocean sunfishes (Family molidae). Bull. Br. Museum Nat. Hist. (Zool.) 1, 87–121.

Genin, A., 2004. Bio-physical coupling in the formation of zooplankton and fish aggregations over abrupt topographies. J. Mar. Syst. 50 (1–2), 3–20.

Graham, W., Pages, F., Hamner, W., 2001. A physical context for gelatinous zooplankton aggregation: a review. Hydrobiologia 451 (1–3), 199–212.
Hartog, J., Hobday, A., Matear, R., Feng, M., 2010. Habitat overlap between southern bluefin tuna and yellowfin tuna in the east coast longline fishery—implications for present and future spatial management. Deep Sea Res. II 58, 746–752.
Hijmans, R., 2015. Raster: geographic data analysis and modeling R package version 2., pp. 4–15 http://CRAN.R-project.org/package=raster.
Hobday, A., Hartog, J., 2014. Derived ocean features for dynamic ocean management. Oceanography 27 (4), 134–145.
International Scientific Committee for Tuna and Tuna-Like Species in the North Pacific Ocean (ISC). 2016. 2016 Pacific Bluefin Tuna Stock Assessment. Annex 9 in Report of the Sixteenth Meeting of the International Scientific Committee on Tuna and Tuna-like Species in the North Pacific Ocean (ISC), 13–18 July, 2016, Sapporo, Japan. 138 p.
Kasperski, S., 2016. Optimal multispecies harvesting in the presence of a nuisance species. Mar. Policy 64, 55–63.
Kitagawa, T., Boustany, A., Farwell, C., Williams, T., Castleton, M., Block, B., 2007. Horizontal and vertical movements of juvenile bluefin tuna (Thunnus orientalis) in relation to seasons and oceanographic conditions in the eastern Pacific Ocean. Fish. Oceanogr. 16 (5), 409–421.
Large, S., Fay, G., Friedland, K., Link, J., 2015. Critical points in ecosystem responses to fishing and environmental pressures. Mar. Ecol. Prog. Ser. 521, 1–17.
Laurs, R., Fiedler, P., Montgomery, D., 1984. Albacore tuna catch distributions relative to environmental features observed from satellites. Deep Sea Res. 31 (9), 1085–1099.
Lewison, R., Hobday, A., Maxwell, S., Hazen, E., Hartog, J., Dunn, D., Briscoe, D., Fossette, S., O'Keefe, C., Barnes, M., Abecassis, M., Bograd, S., Bethony, N., Bailey, H., Wiley, D., Andrews, S., Hazen, L., Crowder, L., 2015. Dynamic ocean management: identifying the critical ingredients of dynamic approaches to ocean resource management. Bioscience 65 (5), 486–498.
Lindegren, M., Mollman, C., Nielsen, A., Stenseth, N., 2009. Preventing the collapse of the Baltic cod stock through an ecosystem-based management approach. Proc. Natl. Acad. Sci. U. S. A. 106 (34), 14722–14727.
Lukacs, P., Burnham, K., Anderson, D., 2010. Model selection bias and Freedman's paradox. Ann. Inst. Stat. Math. 62 (1), 117–125.
Lynn, R., Simpson, J., 1987. The California Current System: the seasonal variability of its physical characteristics. J. Geophys. Res. C 92 (12), 12947–12966.
Macias, D., Landry, M., Gershunov, A., Miller, A., Franks, P., 2012. Climatic control of upwelling variability along the western North-American coast. PLoS One 7 (1), e30436.
Mantua, N., Hare, S., Zhang, Y., Wallace, J., Francis, R., 1997. A Pacific interdecadal climate oscillation with impacts on salmon production. Bull. Am. Meteorol. Soc. 78 (6), 1069–1079.
Martin, S., Stohs, S., Moore, J., 2015. Bayesian inference and assessment for rare-event bycatch in marine fisheries: a drift gillnet fishery case study. Ecol. Appl. 25 (2), 416–429.
Martinez-Rincon, R., Ortega-Garcia, S., Vaca-Rodriguez, J., Griffiths, S., 2015. Development of habitat prediction models to reduce by-catch of sailfish (Istiophorus platypterus) within the purse-seine fishery in the eastern Pacific Ocean. Mar. Freshw. Res. 66 (7), 644–653.
Maxwell, S., Hazen, E., Lewison, R., Dunn, D., Bailey, H., Bograd, S., Briscoe, D., Fossette, S., Hobday, A., Bennett, M., Benson, S., Caldwell, M., Costa, D., Dewar, H., Eguchi, T., Hazen, L., Kohin, S., Sippel, T., Crowder, L., 2015. Dynamic ocean management: defining and conceptualizing real-time management of the ocean. Mar. Policy 58, 42–50.
Miller, I., Scales, K., Ingram, S., Southall, E., Sims, D., 2015. Basking sharks and oceanographic fronts: quantifying associations in the north-east Atlantic. Funct. Ecol. 29 (8), 1099–1109.
Murphy, G., 1959. Effect of water clarity on albacore catches. Limnol. Oceanogr. 4 (1), 86–93.
NMFS. 2016. West Coast Region Observer Program data summaries and reports. http://www.westcoast.fisheries.noaa.gov/fisheries/wc_observer_programs/sw_observer_program_info/data_summ_report_sw_observer_fish.html. (Accessed October 2016).
Nakada, S., Hirose, N., Senjyu, T., Ken-ichi, F., Tsuji, T., Okei, N., 2014. Operational ocean prediction experiments for smart coastal fishing. Prog. Oceanogr. 121, 125–140.
Nakamura, I., Goto, Y., Sato, K., 2015. Ocean sunfish rewarm at the surface after deep excursions to forage for siphonophores. J. Anim. Ecol. 84 (3), 590–603.
Palamara, L., Manderson, J., Kohut, J., Oliver, M., Gray, S., Goff, J., 2012. Improving habitat models by incorporating pelagic measurements from coastal ocean observatories. Mar. Ecol. Prog. Ser. 447, 15–30.
Pebesma, E., Bivand, R., 2005. Classes and methods for spatial data in R. R News 5(2). http://cran.r-project.org/doc/Rnews/.
Pebesma, E., 2004. Multivariable geostatistics in S: the gstat package. Comput. Geosci. 30, 683–691.
Pinkas, L., Oliphant, M., Iverson, I., 1971. Food habits of albacore, bluefin tuna, and bonito in California waters. Fish. Bull. 152, 2–83.
Polovina, J., 1996. Decadal variation in the trans-Pacific migration of northern bluefin tuna (Thunnus thynnus) coherent with climate-induced change in prey abundance. Fish. Oceanogr. 5 (2), 114–119.
Powell, J., Ohman, M., 2015. Covariability of zooplankton gradients with glider-detected density fronts in the southern California Current system. Deep Sea Res. II 112, 79–90.
R Core Team, 2015. R: A Language and Environment for Statistical Computing. R Foundation for Statistical Computing, Vienna, Austria http://www.R-project.org/.
Reiss, C., Checkley, D., Bograd, S., 2008. Remotely sensed spawning habitat of Pacific sardine (Sardinops sagax) and Northern anchovy (Engraulis mordax) within the California Current. Fish. Oceanogr. 17 (2), 126–136.
Sakuramoto, K., 2016. Case study: a simulation model of the spawning stock biomass of Pacific bluefin tuna and evaluation of fisheries regulations. Am. J. Clim. Change 5, 245–260.
Santora, J., Sydeman, W., Schroeder, I., Reiss, C., Wells, B., Field, J., Cossio, A., Loeb, V., 2012. Krill space: a comparative assessment of mesoscale structuring in polar and temperate marine ecosystems. ICES J. Mar. Sci. 69 (7), 1317–1327.
Scales, K., Miller, P., Embling, C., Ingram, S., Pirotta, E., Votier, S., 2014. Mesoscale fronts as foraging habitats: composite front mapping reveals oceanographic drivers of habitat use for a pelagic seabird. J. R. Soc. Interface 11, 20140679.
Silvani, L., Gazo, M., Aguilar, A., 1999. Spanish driftnet fishing and incidental catches in the Mediterranean. Biol. Conserv. 90 (1), 79–85.
Simons R., 2015. ERDDAP. http://coastwatch.pfeg.noaa.gov/erddap. Monterey, CA: NOAA/NMFS/SWFSC/ERD.
Sousa, L., Quieroz, N., Mucientes, G., Humphries, N., Sims, D., 2016. Environmental influence on the seasonal movements of satellite-tracked ocean sunfish Mola mola in the north-east Atlantic. Anim. Biotelem. 4 (7).
Stoner, A., Manderson, J., Pessutti, J., 2001. Spatially explicit analysis of estuarine habitat for juvenile winter flounder: combining generalized additive models and geographic information systems. Mar. Ecol. Prog. Ser. 213, 253–271.
Suchman, C., Brodeur, R., Daly, E., Emmett, R., 2012. Large medusae in surface waters of the Northern California Current: variability in relation to environmental conditions. Hydrobiologia 690 (1), 113–125.
Takano, A., Yamazaki, H., Nagai, T., Honda, O., 2009. A method to estimate three-dimensional thermal structure from satellite altimetry data. J. Atmos. Oceanic Technol. 26 (12), 2655–2664.
Thys, T., Ryan, J., Dewar, H., Perle, C., Lyons, K., O'sullivan, J., Farwell, C., Howard, M., Weng, K., Lavaniegos, B., Gaxiola-Castro, G., Bojorquez, L., Hazen, E., Bograd, S., 2015. Ecology of the ocean sunfish, Mola mola, in the southern California Current system. J. Exp. Mar. Biol. Ecol. 471, 64–76.
Ward, E., Jannot, J., Lee, Y., Ono, K., Shelton, A., Thorston, J., 2015. Using spatiotemporal species distribution models to identify temporally evolving hotspots of species co-occurrence. Ecol. Appl. 25 (8), 2198–2209.
Ware, D., Thomson, R., 2005. Bottom-up ecosystem trophic dynamics determine fish production in the Northeast Pacific. Science 308 (5726), 1280–1284.
Watson, J., Essington, T., Lennert-Cody, C., Hall, M., 2009. Trade-offs in the design of fishery closures: management of silky shark bycatch in the eastern Pacific Ocean tuna fishery. Conserv. Biol. 23 (3), 623–635.
Whitlock, R., Hazen, E., Walli, A., Farwell, C., Bograd, S., Foley, D., Castleton, M., Block, B., 2015. Direct quantification of energy intake in an apex marine predator suggests physiology is a key driver of migrations. Sci. Adv. 1 (8), e1400270.
Whittingham, M., Stephens, P., Bradbury, R., Freckleton, R., 2006. Why do we still use stepwise modelling in ecology and behaviour? J. Anim. Ecol. 75, 1182–1189.
Wood, S., 2006. Generalized Additive Models: An Introduction with R. Chapman & Hall/CRC Press, Boca Raton, FL.
Zhang, C., Chen, Y., Ren, Y., 2016. An evaluation of implementing long-term MSY in ecosystem-based fisheries management: incorporating trophic interaction, bycatch and uncertainty. Fish. Res. 174, 179–189.
Zuur, A., Ieno, E., Walker, N., Saveliev, A., Smith, G., 2009. Mixed Effects Models and Extensions in Ecology with R, 1st ed. Springer, New York.
Zwolinski, J., Demer, D., 2014. Environmental and parental control of Pacific sardine (Sardinops sagax) recruitment. ICES J. Mar. Sci. 71 (8), 2198–2207.
Zydelis, R., Lewison, R., Schaffer, S., Moore, J., Boustany, A., Roberts, J., Sims, M., Dunn, D., Best, B., Tremblay, Y., Kappes, M., Halpin, P., Costa, D., Crowder, L., 2011. Dynamic habitat models: using telemetry to project fisheries bycatch. Proc. R. Soc. B 278 (1722), 3191–3200.